Computer Physics Communications 180 (2009) 1382–1391

Contents lists available at ScienceDirect

Computer Physics Communications

www.elsevier.com/locate/cpc

Coding coarse grained polymer model for LAMMPS and its application to polymer crystallization[☆]

Chuanfu Luo[a,*], Jens-Uwe Sommer[a,b]

[a] *Leibniz-Institut für Polymerforschung Dresden, D-01069 Dresden, Germany*
[b] *Technische Universität Dresden, Institute for Theoretical Physics, Zellescher Weg 17, D-01069 Dresden, Germany*

ARTICLE INFO

Article history:
Received 11 July 2008
Received in revised form 18 January 2009
Accepted 30 January 2009
Available online 7 February 2009

PACS:
61.20.Ja
61.25.H-
61.41.+e
68.55.am
82.35.Lr

Keywords:
Molecular dynamics (MD)
Coarse grained polymer model
LAMMPS
Polymer crystallization
Parallel computing

ABSTRACT

We present a patch code for LAMMPS to implement a coarse grained (CG) model of poly(vinyl alcohol) (PVA). LAMMPS is a powerful molecular dynamics (MD) simulator developed at Sandia National Laboratories. Our patch code implements tabulated angular potential and Lennard-Jones-9-6 (LJ96) style interaction for PVA. Benefited from the excellent parallel efficiency of LAMMPS, our patch code is suitable for large-scale simulations.

This CG-PVA code is used to study polymer crystallization, which is a long-standing unsolved problem in polymer physics. By using parallel computing, cooling and heating processes for long chains are simulated. The results show that chain-folded structures resembling the lamellae of polymer crystals are formed during the cooling process. The evolution of the static structure factor during the crystallization transition indicates that long-range density order appears before local crystalline packing. This is consistent with some experimental observations by small/wide angle X-ray scattering (SAXS/WAXS). During the heating process, it is found that the crystalline regions are still growing until they are fully melted, which can be confirmed by the evolution both of the static structure factor and average stem length formed by the chains. This two-stage behavior indicates that melting of polymer crystals is far from thermodynamic equilibrium. Our results concur with various experiments. It is the first time that such growth/reorganization behavior is clearly observed by MD simulations.

Our code can be easily used to model other type of polymers by providing a file containing the tabulated angle potential data and a set of appropriate parameters.

Program summary

Program title: lammps-cgpva
Catalogue identifier: AEDE_v1_0
Program summary URL: http://cpc.cs.qub.ac.uk/summaries/AEDE_v1_0.html
Program obtainable from: CPC Program Library, Queen's University, Belfast, N. Ireland
Licensing provisions: GNU's GPL
No. of lines in distributed program, including test data, etc.: 940 798
No. of bytes in distributed program, including test data, etc.: 12 536 245
Distribution format: tar.gz
Programming language: C++/MPI
Computer: Tested on Intel-x86 and AMD64 architectures. Should run on any architecture providing a C++ compiler
Operating system: Tested under Linux. Any other OS with C++ compiler and MPI library should suffice
Has the code been vectorized or parallelized?: Yes
RAM: Depends on system size and how many CPUs are used
Classification: 7.7
External routines: LAMMPS (http://lammps.sandia.gov/), FFTW (http://www.fftw.org/)
Nature of problem: Implementing special tabular angle potentials and Lennard-Jones-9-6 style interactions of a coarse grained polymer model for LAMMPS code.
Solution method: Cubic spline interpolation of input tabulated angle potential data.

[☆] This paper and its associated computer program are available via the Computer Physics Communications homepage on ScienceDirect (http://www.sciencedirect.com/science/journal/00104655).

[*] Corresponding author.
E-mail addresses: luochuanfu@gmail.com, luo@ipfdd.de (C. Luo).

doi:10.1016/j.cpc.2009.01.028

Restrictions: The code is based on a former version of LAMMPS.
Unusual features.: Any special angular potential can be used if it can be tabulated.
Running time: Seconds to weeks, depending on system size, speed of CPU and how many CPUs are used. The test run provided with the package takes about 5 minutes on 4 AMD's opteron (2.6 GHz) CPUs.
References:

[1] D. Reith, H. Meyer, F. Müller-Plathe, Macromolecules 34 (2001) 2335–2345.
[2] H. Meyer, F. Müller-Plathe, J. Chem. Phys. 115 (2001) 7807.
[3] H. Meyer, F. Müller-Plathe, Macromolecules 35 (2002) 1241–1252.

1. Introduction

When polymers that are sufficiently regular (little branching, stereo-regularity, such as polyethylene (PE), poly(vinyl alcohol) (PVA), etc.) are cooled from a temperature above the melting point to the crystallization temperature, polymer crystals tend to be formed. The resulting structure is semicrystalline, containing both amorphous and crystalline regions. The crystalline regions consist of lamellar sheets in which the polymers are folded back and forth on themselves. The lamellae are stacked and finally form so-called spherulites. This hierarchy of morphological features involve different length scales, ranging from nanoscopic level (atoms, molecules, <5 nm) over intermediate-sized structure (chains, lamellae, 5–50 nm), to macroscopic spherulites (>500 nm) [1–3].

Polymer crystallization is a classical problem of polymer research and of great technological and scientific importance. Although it has been studied experimentally for many years, a consistent theoretical model has not yet been developed [1–20]. The difficulty lies in the fact that crystalline polymers are far from thermodynamic equilibrium. Further more, recent experimental studies give strong indication for a multi-stage process where the polymer chains undergo conformational transitions before an overall crystalline phase is developed. However, experimental observations such as X-ray scattering depend on the sensitivity of detectors and it is difficult to observe the dynamics of individual polymer chains during the various stages of polymer crystallization.

Computer simulations generally have two advantages which may help to understand the non-equilibrium process of polymer crystallization: First, the trajectories of all particles are available, giving information about single molecules which are not easily accessible by experiments. Second, models of variable complexity can be simulated. Thus we can adjust parameters successively to investigate the effect of certain interactions separated from others.

There are several simulation methods suitable for the study of polymers, which are intimately connected to the probed length scale. The most "accurate" method is the *ab initio* calculation, however it requires a huge amount of computer time and cannot be used to study the process of polymer crystallization. The most "effective" method is the finite-element simulation. It is useful to understand the macroscopic properties of a material, but its length scale is too large and does not permit a resolution of the positions of different polymer chains in the case of polymer crystallization. Thus, only intermediate solutions between these two schemes are appropriate for the study of polymer crystallization, i.e. the relevant simulation methods are situated on the atomic (all-atom model) or molecular level (united-atom or coarse-grained model). All atom simulations of polymers suffer from the detailed treatment of the fast modes (e.g., C–H bond vibrations) on the microscopic length scale. It has the serious consequence that the time propagation of the system can only be performed in tiny steps. Consequently, the slow modes (e.g., radius of gyration or end-to-end vector) can hardly be equilibrated. It is therefore not feasible to derive specific macroscopic bulk properties of polymers. United-atom or coarse-grained models can provide reasonable resolution and also are effective to perform computer simulations, so they are widely used to study polymer crystallization [18,21–24]. However, polymer crystallization processes are rather slow on the molecular time scale and its' simulations require efficient parallel computing.

2. CG-PVA model

Recently, Meyer and Müller-Plathe developed a simplified model for PVA derived by a systematic coarse-graining procedure [25–29]. In their CG-PVA model, a coarse-grained bead represents one monomeric unit of PVA. It is unlike from commonly used united-atom (UA) models, which consider one bead as a carbon and its nearby small atoms. In the CG-PVA model, the beads are connected by harmonic springs, and additionally interact by an angle bending potential retaining information on the torsional states of the atomistic backbone. The non-bonded interactions are approximated by a Lennard-Jones-9-6 (LJ96) potential. Furthermore, for the simulation of a dense melt, it is sufficient to take only the repulsive part of the potential [30]. This leads to some shift of energy and pressure while it affects only a little the qualitative behavior of the system. This approximation speeds up the simulation.

The key idea of the CG-PVA model is to map the *torsional potential* of backbones to the angular *bending potential* in bead-spring model. The length scales are fixed by mapping from atomistic simulations. The length unit is $\sigma = 1 = 0.52$ nm, corresponding roughly to the chain diameter of PVA. The bond length is $b_0 = 0.5 = 0.26$ nm. Temperatures and energies are expressed in reduced units with $m = k_B = 1$ (mass, Boltzmann's constant). The value of the temperature $T = 1$ corresponds to 550 K (the high-temperature phase of the amorphous melt). The time unit is estimated as $\tau = 1.63$ ps.[1] In these units, the density is about 2.1 monomers per σ^3.

The non-bonded potential between monomers is given by LJ96 interactions:

$$U_{nonb}(r) = \varepsilon\left(\left(\frac{\sigma_0}{r}\right)^9 - \left(\frac{\sigma_0}{r}\right)^6\right), \tag{1}$$

[1] It is hard to accurately map the time unit to real time. Monomers in CG-PVA model are much more regular and smoother than real monomers. In principle, the dynamics of CG-PVA model should be faster than that of real polymer chains. This estimated real time is just by the convert relation of units and it should be underestimated.

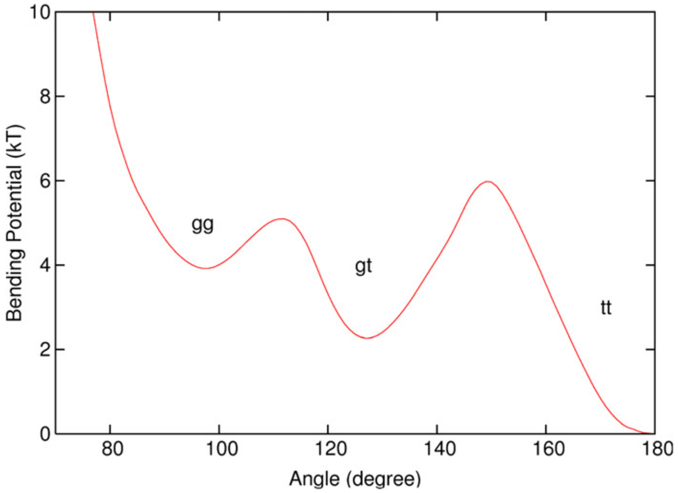

Fig. 1. Bending (angular) potential of CG-PVA model. The minimum "tt" at 180° corresponds to two successive trans torsion on the atomistic backbone. The minima "gg" and "gt" correspond to gauche–gauche and gauche–trans sequences, respectively.

where r is the distance between two monomers, $\varepsilon = 1.511 k_B T$, and $\sigma_0 = 0.89\sigma$. This potential is cut off at the distance $r_{cut} = 1.02\sigma$, where $U_{nonb}(r)$ reaches its minimum.

Both the binding and angular potentials are derived from the distributions of bond lengths and torsion angles of atomistic simulations by the inverse Boltzmann method:

$$U_{bond}(r) = -k_B T \ln\bigl[P(r)\bigr], \tag{2}$$

and

$$U_{ang}(\theta) = -k_B T \ln\bigl[P(\theta)/\sin(\theta)\bigr], \tag{3}$$

where r is the bond length and θ is the bending angle. $P(r)$ and $P(\theta)$ are distributions of bond lengths and bending angles, respectively. By mapping all atom simulations, the final bond potential is given by

$$U_{bond}(r) = \frac{1}{2} k_{bond} (r - b_0)^2, \tag{4}$$

where $b_0 = 0.5\sigma$, and $k_{bond} = 2704 k_B T/\sigma^2$. The final angular potential is a tabulated potential as show in Fig. 1. It has three minima corresponding to three different states of the original torsion potential of backbones, which are trans–trans state at 180°, trans–gauche state at near 120°, and gauche–gauche state at near 100°.

3. LAMMPS and CG-PVA patch code

Computer simulations have been used to address various aspects of polymer crystallization: Monte-Carlo (MC) simulations on a lattice were applied to model the selection of lamellar thickness in the crystal [31–33], which requires the hypothesis that a growth front preexists between the crystalline and amorphous regions. Direct molecular dynamics (MD) simulations have been applied to short chains in the melt and clusters in vacuum or thin films [21–24]. MD simulations give more realistic and reliable crystallization process as compared to MC simulations, for they do not introduce any artificial hypothesis about the dynamics. LAMMPS [34] is a powerful MD simulator developed at Sandia National Lab, and it is a free software and distributed under the GNU general public licence (GPL). It is designed for large scale and massively parallel simulations and the code is easy to modify or extend with new functionality. It uses spatial decomposition techniques to partition the simulation domain into small 3D sub-domains, one of which is assigned to each processor. The communication between different processors is realized by using Message Passing Interface (MPI). This allows it to run large systems in a scalable way wherein both memory and execution speed linearly scale with the number of atoms being simulated.

To apply the CG-PVA model to LAMMPS, we need to write a patch code to add the special LJ96 pair potential and the tabular angle potential. For the original angle potential from Eq. (3) is in form of discrete value pairs, we use the cubic spline interpolation to smooth both the potentials and forces. The final code is suitable for large scale simulations. Our current code is based on the 22Jun2007 version of LAMMPS.

Following the spirit of how the CG-PVA is derived [27], it is not difficult to develop other coarse-grained models for polymers such as polyethylene (PE). We think our patch code is much useful and convenient for who are interested in this field, so we are going to put our patch code to public domain and describe how to use it here.[2]

4. How to

In order to use our patch code, you need to copy the five source files to the "src" directory of LAMMPS and then compile them as you compile LAMMPS. Then you will get an executable file which we will refer to as "lammps". Generally, there are two files needed to run a

[2] We are going to contact the developer of LAMMPS, so later version of LAMMPS may contain our patch code.

LAMMPS simulation job: the initial structure file and the job script input file. To use the tabular angle potential of CG-PVA, a tabular file which contains the tabulated angular potential is also needed. Then you can run it as run usual LAMMPS jobs, like this (may be a little different on different MPI implementation environment):

```
mpirun -np 4./lammps < test.in
```

Here is an example input script file:

```
#filename:"test.in",  this is an example input file

units lj              #use reduced units

atomstyle angle       #set potential style
readdata poly.data          #initial data file

pairstyle lj96/cut 1.02     #set LJ style and cutoff
pairmodify shift yes        #shift energy at cutoff
paircoeff 1 1 0.37775 0.89  #set LJ parameters

bondstyle harmonic        #set bond style
bondcoeff 1 1352.0 0.5    #set bond parameters

anglestyle table spline 181     #set angle style
anglecoeff 1 cgpva.table CGPVA  #CGPVA angular potential file

specialbonds 0 0 1.0 #exclude 1-1,1-2 neighbors' LJ interaction

restart 1000000 poly.restart      #restart file
dump 1 all atom 100000 poly.dump  #dump file
dumpmodify 1 image yes scale no   #dump image values

thermo 100         #interval of statistic information
timestep 0.01      #MD time step
fix 1 all npt 1.0 0.6 1.0 xyz 8.0 8.0 10.0 #NPT & quench
run 40000      #total MD steps
```

Most commands are the same as LAMMPS input script file which are well documented in the manual of LAMMPS. What we should note here is the “pair_style”, “pair_coeff”, “angle_style”, and “angle_coeff” command lines. We will specify the syntax in details as follows:

```
anglestyle table <style> <N>
anglecoeff <type> <filename> <keyword>
```

These two lines specify the tabular angle potential. Where the < style > is “linear” or “spline”, it is the method of interpolation. < N > means using *N* values in tables. The whole scope of interval from 0 to 180 degrees will be evenly divided by *N* points. The < type > is the atom type specified to use the tabular potential, which is 1 in our example input. The < filename > is the name of the tabulated angle potential file, which format will be introduced later. The < keyword > is the identity of a certain tabular values, which is CGPVA in our example input file.

The key word “anglestyle table” creates interpolation tables of length *N* from angular potential and force values listed in a file(s) as a function of degree. The files are read by the “angle_coeff” command. The interpolation tables are created by fitting cubic splines to the file values and interpolating energy and force values at each of *N* distances. During a simulation, these tables are used to interpolate energy and force values as needed. The interpolation is done in one of two styles: “linear” or “spline”. For the “linear” style, the angle is used to find two surrounding table values from which an energy or force is computed by linear interpolation. For the “spline” style, a set of cubic spline coefficients are computed and stored for each of the *N* values in the table. The angle is used to find the appropriate set of coefficients which are used to evaluate a cubic polynomial which computes the energy or force.

The following coefficients must be defined for each pair of atoms types via the “angle_coeff” command as in the example above, or in the data file or restart file read by the “read_data” or “read_restart” commands: < filename > and < keyword >. The < filename > specifies a file containing tabulated energy and force values. The < keyword > specifies a section of the file.

The format of a tabulated file is as follows (without the parenthesized comments):

```
#Angle potential for CG-PVA (one or more comment or blank lines)
#Col-1: index
#Col-2: angle  (degree)
#Col-3: energy (LAMMPS unit)
#Col-4: force  (LAMMPS unit/degree)

CGPVA        (keyword is the first text on line)
N 181 FP 0 0 (N, FP parameters)
                             (blank line)
```

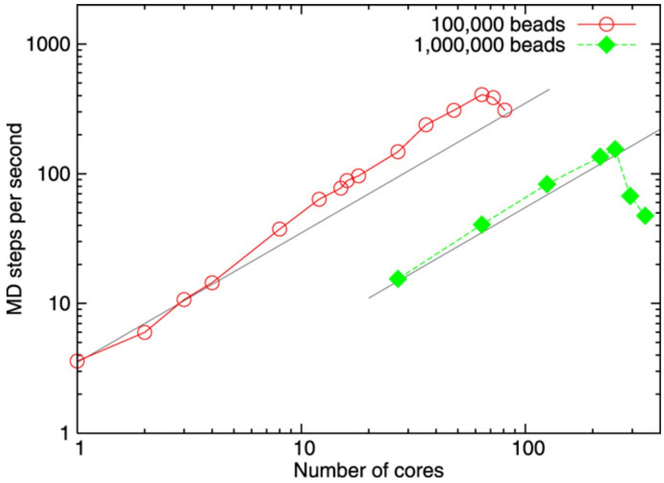

Fig. 2. Scaling performances of two example systems consisting of 1×10^5 and 1×10^6 beads. The dashed lines indicate linear scaling performance.

```
1 0.0 200.5 2.5            (index, angle, energy, force)
2 1.0 198.0 2.5
...
181 180.0 0.0 0.0
```

A section begins with a non-blank line whose first character is not a “#”. Blank lines or lines starting with “#” can be used as comments between sections. The first line of a section begins with a keyword which identifies the section. The line can contain additional text, but the initial text must match the argument specified in the angle_coeff command. The next line lists (in any order) one or more parameters for the table. Each parameter is a keyword followed by one or more numeric values. The parameter “N” is required and its value is the number of table entries that follow. The “FP” parameter is optional. If used, the parameter “FP” is followed by two values fplo and fphi, which are the derivative of the force at the innermost and outermost angles (0° and 180°). These values are needed by the spline construction routines. If not specified by the “FP” parameter, they are estimated (less accurately) by the first two and last two force values in the table.

Following a blank line, the next N lines list the tabulated values. On each line, the first value is the index from 1 to N, the second is the angle value (in degree), the third is the energy (in energy unit), and the fourth is the force (in force unit). The angle values must increase from one line to the next, and it should be from 0 to 180.

Note that one file can contain many sections, each with a tabulated potential. LAMMPS reads the file section by section until it finds one that matches the specified keyword. Otherwise, an error message will be given.

This angle style writes the settings for the “angle_style table” command to binary restart files, so a angle_style command does not need to specified in an input script that reads a restart file. However, the coefficient information is not stored in the restart file, since it is tabulated in the potential files. Thus, pair_coeff commands do need to be specified in the restart input script.

5. Parallel efficiency

Our patch code for LAMMPS is designed for large-scale simulations, so the parallel efficiency is important. Here, we give an example for the “upscaling” performance on our Linux PC cluster using a system consisting of 200 polymer chains each of length 500 (totally 1×10^5 beads). The hardware configurations are dual-core AMD opteron(tm) processors 8218 (2.6 GHz) connected by infiniband network. The performance on different number of CPUs (cores) is shown in Fig. 2. The best performance is achieved at 64 CPUs (117 times faster than 1 CPU). The parallel efficiency is above linear scaling at 8–64 CPUs. The reason probably is that smaller memory on each core has faster cache performance. When number of cores larger than 64 is used, the performance is decreased for network latency. A larger system consisting 1 million beads (1000 polymer chains each of length 1000) was tested on the super computer at ZIH of the Technische Universität Dresden [35], using AMD’s 2.6 GHz opteron processors connected by infiniband network. The performance is also shown in Fig. 2, from which the best performance for this larger system is found to be achieved at 252 CPUs.

We conclude that our patch code displays a good parallel performance and the optimal number of cores can be determined depending on system size.

6. Application to polymer crystallization

6.1. Computational method

This CG-PVA code is applied to simulate polymer crystallization processes. The simulated system we will discuss in the following contains 200 polymers and each polymer chain consists of 500 beads (repeat units or PVA monomers), so the total number of beads is 1×10^5. The initial structure of the system is prepared by self-avoiding random walks. This initial structure is first relaxed at $T = 1.0$ far above melting point by 6×10^7 MD steps to ensure the structure to be fully relaxed. The relaxed system is cooled from $T = 1.0$ to 0.6 by 4×10^7 MD steps (the cooling rate is $1 \times 10^{-6}\tau^{-1}$), followed by a heating process to $T = 1.0$ at the same rate. The time step of integration is 0.01τ. Periodic boundary condition and NPT ensemble are used during the simulations, and the pressure is set to be 8 (corresponding

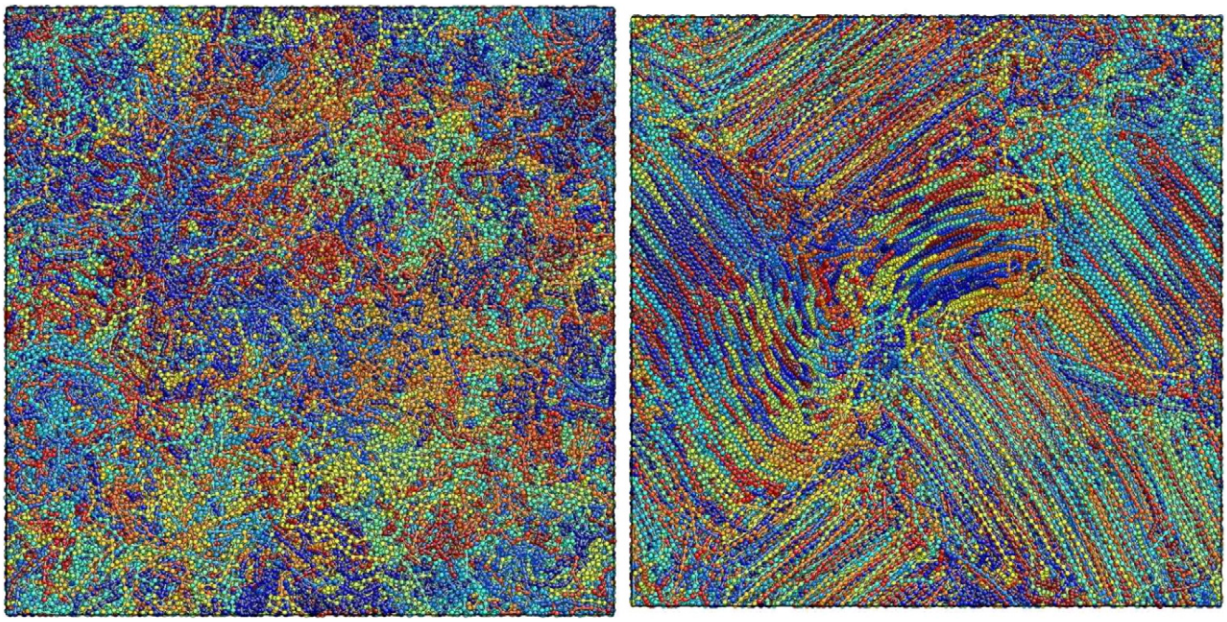

Fig. 3. Snapshots of the polymer system at $T = 1.0$ (left) and $T = 0.6$ (right). Here different colors denote different chains. The size of box at $T = 0.6$ is smaller than that at $T = 1.0$. Polymer chains are randomly coiled at $T = 1.0$. At $T = 0.6$, most chains are straightly folded and aligned together, but there are still some regions where chains are kept coiled structure as shown at the top-right corner of the figure. (For interpretation of the references to color in this figure legend, the reader is referred to the web version of this article.)

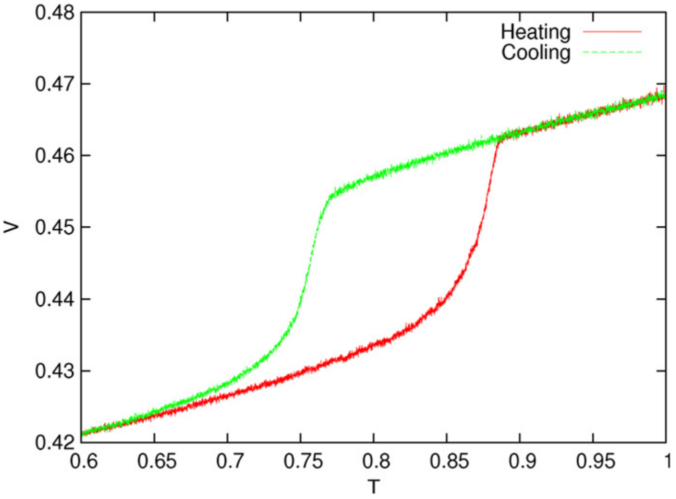

Fig. 4. Volume per bead versus temperature during the heating/cooling cycle. The drop/jump of volume indicates the phase transition.

to 1 atm). The pressure is kept constant through a Brendsen barostat and the parameter of damp time is 1000 MD steps. The temperature is controlled by Nosé–Hoover thermostat and the parameter of damp time is 100 MD steps. By using parallel computation on 64 CPUs, the time needed for each cooling/heating process is about 32 hours.

6.2. Results and discussions

The system undergoes a phase transition when it is cooled from $T = 1.0$ to $T = 0.6$. At $T = 1.0$, the system is liquid melt and polymer chains are randomly coiled as shown in the left of Fig. 3, While at lower temperature $T = 0.6$, the system is crystallized. A snapshot of the structure at $T = 0.6$ is given in the right of Fig. 3. Here, most polymer chains are folded forth and back, and aligned together to form a crystalline structure. However, there are still some amorphous regions in which polymer chains have a coiled structure. This kind of structure is a typical crystalline state of polymer system, so-called "semi-crystalline" state. We note here that the simulation time in our case is still not enough to develop rather extended "lamellar" structure as observed in experiments. However, the Gibbs–Thomson-like relation which is observed in many experiments, can be obtained using the present CG-PVA model [25,26].

From Fig. 3, it is obvious that the box size at $T = 0.6$ is smaller than that at $T = 1.0$. The density jump is related to the phase transition from liquid to crystalline state. In Fig. 4, we display the volume per bead (V) as a function of temperature during the cooling/heating cycle. The volume decreases with temperature and a sudden drop/jump of the volume is attributed to a phase transition. The obvious hysteresis of the cooling and heating cycle indicates that the crystallization and melting processes of polymers are far from thermody-

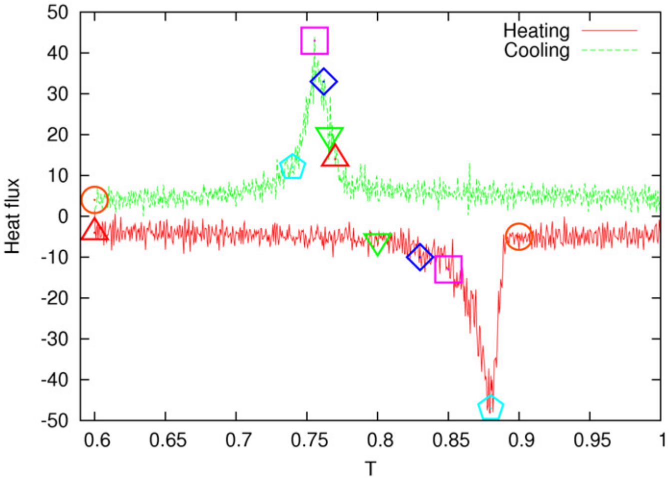

Fig. 5. Heat flux out from the system versus temperature during the heating/cooling cycle. The peaks indicate phase transition temperatures. The marked points on the cooling and heating lines are some special temperatures where their static structure factors are calculated and shown in Figs. 6 and 7.

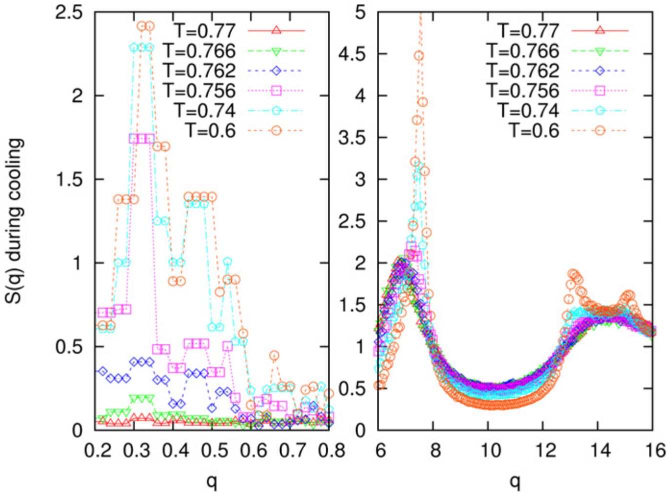

Fig. 6. Evolution of static structure factor during cooling process. The peak at small q region appears before Bragg peaks (large q region). Various temperatures are indicated with corresponding symbols in Fig. 5.

namic equilibrium. From the drop/jump point of volume, we can estimate the crystallization temperature $T_c \sim 0.75$–0.77 and the melting temperature $T_m \sim 0.88$–0.89.

In experiments, heat flux can be measured by calorimetry and the apparent non-equilibrium crystallization and melting temperatures can be determined. The heat flux dQ in MD simulations can be calculated by the first law of thermodynamics as $dQ = dU + p\,dV$, where the changes of energy dU and volume dV can be directly calculated from MD simulations. The heat flux out from the simulated system is given in Fig. 5. The peaks of heat flux can be associated with phase transitions as the drop/jump of volume. The values of $T_c = 0.756$ and $T_m = 0.88$ (peaks of heat flux) are within the estimated temperature scopes from V–T curves in Fig. 4. We note at this point that crystallization and melting processes far from thermodynamic equilibrium may be very different from those at equilibrium.

A quantity that permits a direct link to experiments is the static structure factor, which can be measured by neutron or X-ray scattering. The static structure factor $S(\vec{q})$ is defined as:

$$S(\vec{q}) = \frac{1}{N}\langle \rho(\vec{q})^* \rho(\vec{q})\rangle, \tag{5}$$

where N is the total number of beads in the system, and $\rho(\vec{q})$ is the Fourier transformation of the density function $\rho(\vec{r}) = \sum_{j=1}^{N} \delta(\vec{r} - \vec{r}_j)$:

$$\rho(\vec{q}) = \int \rho(\vec{r}) e^{-i\vec{q}\cdot\vec{r}}\, d\vec{r} = \sum_{j=1}^{N} e^{-i\vec{q}\cdot\vec{r}_j}. \tag{6}$$

For an isotropic system, $S(\vec{q})$ reduces to $S(q)$ [36]. With periodic boundary conditions, the minimum available wave vector is $q_L = 2\pi/L$, where L is the size of cubic box.

We display the $S(q)$ during the cooling process in Fig. 6. Here, we separate $S(q)$ into two parts of the small q (< 1) and large q (> 5) regions. The small q region can be obtained in small angle scattering experiments (for instance SAXS–small angle X-ray scattering), while the large q region is obtained by wide angle scattering methods such as WAXS. At small q, only few wave vectors enter the average, and

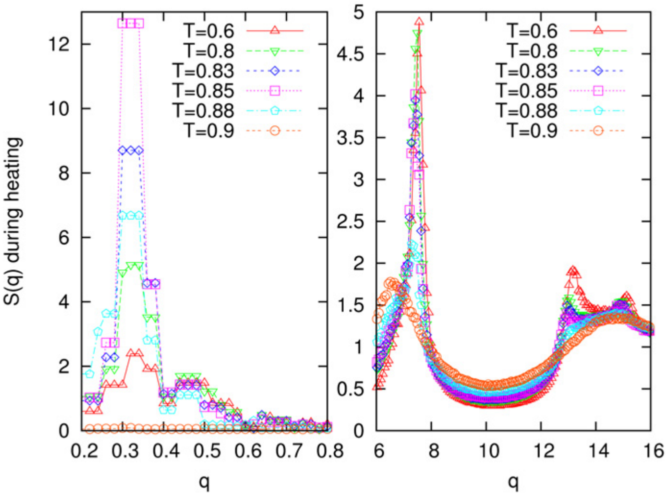

Fig. 7. Evolution of static structure factor during heating process. The peak at small q region is still growing until $T = 0.85$ and its location is shifted to even smaller q, see Fig. 5 for the location of temperatures in the heating process.

the precision is not as good as for larger values of q. However, the peak in $S(q)$ at small q region is well compatible with the average thickness of the lamellar-like structures calculated by the intra-chain bond orientation correlation function, which we will discuss later.

From the $S(q)$ during cooling process in Fig. 6, it is found that at higher temperatures until $T = 0.77$ the system is in liquid state. $S(q)$ has no obvious peak at low q region and it is smooth at higher q region, which is a typical liquid scattering behavior. When the system is cooled down to $T = 0.766$, a small peak of $S(q)$ appears near $q = 0.3$ while there is no change at higher q region. With cooling down of temperature, the peak at small q grows steadily and there is no obvious change at higher q until down to $T = 0.756$. The peak at small q region has grown very obvious while the location of the smooth peak of $S(q)$ near $q = 7$ has a little shift toward to higher q (the first Bragg peak, $q \cong 7.5$). The $S(q)$ is still smooth at $q = 12$–16. Similar simulation results have been reported in Ref. [18], however, using a very stiff chain model. At a temperature of 0.74, the peaks of $S(q)$ at low q and the first Bragg peak ($q \cong 7.5$) has grown very sharp, and the second and third Bragg peaks also can be recognized. Note that the shift of the peak toward higher q values corresponds to the density jump during solidification. Comparing with the volume and heat flux shown in Figs. 3 and 4, we think that the main transition from liquid melt to solid crystalline has finished at $T = 0.74$. This process can be followed in Fig. 5: Crystalline order emerges only at the peak position ($T = 0.756$). The right shoulder of the crystallization exotherm seems to be associated with a pre-ordering process. The crystalline structure is established only at the end of the left shoulder of the crystallization exotherm ($T = 0.74$).

When the temperature is cooled down further, the crystal grows further and the structure is becoming more regular. Both the low q peak and the first three Bragg peaks of $S(q)$ at $T = 0.6$ are clearly developed, and the intensity is also larger as compared to that at $T = 0.74$.

During the heating process, $S(q)$ does not behave inversely with respect to the cooling process. Fig. 7 displays the evolution of $S(q)$ during the heating process. It is found that from $T = 0.6$ to $T = 0.85$, the intensity of the peak at low q is *increased*, while the location of first Bragg peak does not change. The second and third Bragg peaks changes a little, but the peaks are still obvious. In the same time, the location of the peak at low q region has a slight shift to lower q. Thus, the system is still in crystalline state and the crystallization fraction and the thickness of lamellae structure is growing, which is a process corresponding to crystal growth not to melting. This illustrates the non-equilibrium nature of polymer crystals: When temperature is increased (but still below the melting point), the mobility of polymer chains is increased. As a consequence the free energy barrier for forming new crystals and for reorganizing crystalline domains are decreased. This reorganization process is rather slow and is observed in a slow heating process only. In former simulation works, reorganization is reported after a long time under constant temperature. This is the first time that reorganization is observed during continuously heating by computer simulations. When temperature reaches up to $T = 0.88$ the system starts melting. The intensities of peak at low q region and the first Bragg peak are decreased, and the second and third Bragg peaks is beginning to disappear. The system is fully melted at $T = 0.9$, where all peaks of $S(q)$ disappear and are smooth as liquid.

The reorganization process can be shown more clearly by the average stem length of polymer chains, which can be estimated by the intra-chain bond orientation correlation function, $P_1(k)$. The $P_1(k)$ is defined by

$$P_1(k) = \langle \hat{b}_j \cdot \hat{b}_{j+k} \rangle_j, \tag{7}$$

where $\hat{b}_j$ is the unit vector of bond vector $\vec{b}_j$, and the average is taken over all bonds. In crystalline state, $P_1(k)$ usually is an oscillatory function and it can be used to determine the stem length: Once the chains fold, *anti-correlations* occur that correspond to two bonds lying antiparallel to each other (hairpins). The measurement of the first minimum of $P_1(k)$ gives an estimated average value for the stem length of polymer chains.

Fig. 8 shows the evolution of estimated average stem length, d, during cooling and heating cycle. During the cooling process, the average stem length jumps at $T \cong 0.76$, which is corresponding to the appearance peak of the $S(q)$ at small q region, see Fig. 6. Then d is increased up to 17.5 with the decrease of temperature. The average stem length is kept almost 17.5 when $T < 0.7$. The corresponding wave vector is $2\pi/d = 0.36$, which is comparable with the first peak of $S(q)$ appears at $q = 0.3$–0.35. During the heating process, it is obvious that the average stem length is *increased* from $d = 17.5$ at $T = 0.7$ to $d = 21$ at $T \cong 0.88$. The stem length then drops at $T \cong 0.89$–0.9, which is corresponds to the point where all peaks of $S(q)$ disappear. This growth behavior during the heating process indicates that the polymer melting process is far from thermodynamic equilibrium, and is consistent with experimental observations of multi-stage melting [37–42].

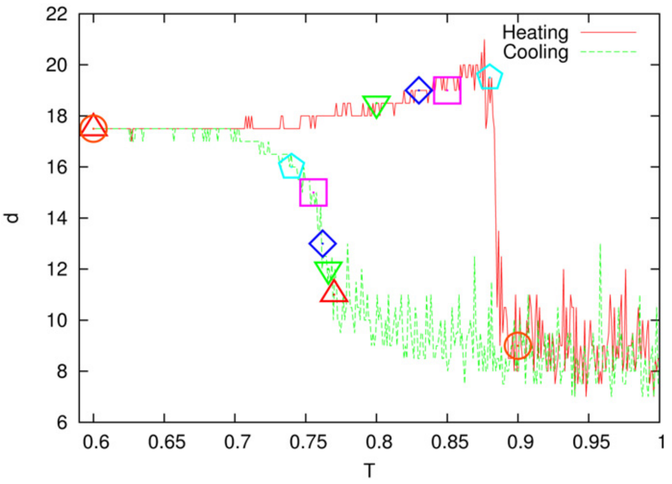

Fig. 8. Evolution of estimated average stem length during cooling/heating cycle. It is clear that from near $T = 0.7$ to $T \cong 0.88$ during the heating process, the average stem length is growing with the increase of temperature. The marked points are the same as in Fig. 5 and the symbols correspond to those in Figs. 6 and 7.

What is the thicken mechanism during the heating? One possible explanation is the increase of chain mobility. When temperature is heated up to a certain value, the free energy barrier for chain movement is lowered and the chains can move easier. If some of folded polymer chains with longer stem length can withstand such a higher temperature (with higher melting temperature), they may keeps growing rather than melting because that the energy of longer stem length is lower. However, the real reason needs more detailed studies of individual chains and also needs more simulations data with larger system and longer simulation time.

7. Conclusions

A patch code for LAMMPS to implement a coarse grained polymer model of poly (vinyl alcohol) is developed. The details of the model, it's implementation for LAMMPS, and how to use the code are described in this paper. The code is tested under Linux system with MPI parallel environment, and it displays excellent parallel efficiency on PC clusters.

The code is used to study polymer crystallization process. With the power of parallel computing, rather slow cooling and heating processes for long chains can be simulated. The evolution of the static structure factor is calculated during the cooling and heating process. During the cooling process, it is found that the peak at small q region appears before the Bragg peaks at large q regions. This result is consistent with some experimental observations. We note that in computer simulation the results for larger q values are easy to obtain and are less error-prone. During the heating process, it is found that the intensity of the peak at small q regions are still growing before the system is fully melted. The evolution of average stem length of polymer chains also shows that the stem length is growing before the system is melted. Such growth of stem length during a heating process is the first time observed by computer simulations.

Acknowledgements

We thank Hendrik Meyer for his kindly supply of original tabulated angle potential data of CG-PVA and helpful discussion.

References

[1] J.-U. Sommer, G. Reiter (Eds.), Polymer Crystallization: Observations, Concepts and Interpretations, Lecture Notes in Physics, vol. 606, Springer, Berlin, 2003.
[2] G. Strobl, The Physics of Polymers, 3rd edition, Springer, Berlin, 2007.
[3] G. Reiter, G. Strobl (Eds.), Progress in Understanding of Polymer Crystallization, Lecture Notes in Physics, vol. 714, Springer, Berlin, 2007.
[4] E.W. Fischer, Stufenförmiges und spiralförmiges wachstum bei hochpolymeren, Z. Naturf. A 12 (9) (1957) 753–754.
[5] A. Keller, A note on single crystals in polymers – evidence for a folded chain configuration, Phil. Mag. 2 (21) (1957) 1171–1175.
[6] P.H. Till, The growth of single crystals of linear polyethylene, J. Polym. Sci. 24 (106) (1957) 301–306.
[7] J.D. Hoffmann, G.T. Davis, J.I. Lauritzen, The Rate of Crystallization of Linear Polymers with Chain Folding, in: Treatise in Solid State Chemistry, vol. 3, Plenum Press, 1976, pp. 497–614.
[8] D.M. Sadler, G.H. Gilmer, Rate-theory model of polymer crystallization, Phys. Rev. Lett. 56 (25) (1986) 2708.
[9] D.M. Sadler, New explanation for chain folding in polymers, Nature 326 (1987) 174–177.
[10] G. Reiter, G. Castelein, J.-U. Sommer, A. Röttele, T. Thurn-Albrecht, Direct visualization of random crystallization and melting in arrays of nanometer-size polymer crystals, Phys. Rev. Lett. 87 (22) (2001) 226101.
[11] A. Röttele, T. Thurn-Albrecht, J.-U. Sommer, G. Reiter, Thermodynamics of formation, reorganization, and melting of confined nanometer-sized polymer crystals, Macromolecules 36 (4) (2003) 1257–1260.
[12] P.D. Olmsted, W.C.K. Poon, T.C.B. McLeish, N.J. Terrill, A.J. Ryan, Spinodal-assisted crystallization in polymer melts, Phys. Rev. Lett. 81 (2) (1998) 373–376.
[13] G. Strobl, From the melt via mesomorphic and granular crystalline layers to lamellar crystallites: A major route followed in polymer crystallization? Eur. Phys. J. E 3 (2) (2000) 165–183.
[14] P. Welch, M. Muthukumar, Molecular mechanisms of polymer crystallization from solution, Phys. Rev. Lett. 87 (21) (2001) 218302.
[15] M. Muthukumar, Modeling polymer crystallization, Adv. Pol. Sci 191 (2005) 241–274.
[16] W. Hu, T. Albrecht, G. Strobl, Reversible surface melting of PE and PEO crystallites indicated by TMDSC, Macromolecules 32 (22) (1999) 7548–7554.
[17] W. Hu, D. Frenkel, V.B.F. Mathot, Intramolecular nucleation model for polymer crystallization, Macromolecules 36 (21) (2003) 8178–8183.
[18] R.H. Gee, N.M. Lacevic, L.E. Fried, Atomistic simulations of spinodal phase separation preceding polymer crystallization, Nature Materials 5 (2006) 39–43.
[19] E.B. Sirota, Polymer crystallization: Metastable mesophases and morphology, Macromolecules 40 (4) (2007) 1043–1048.
[20] M. Soccio, A. Nogales, N. Lotti, A. Munari, T.A. Ezquerra, Evidence of early stage precursors of polymer crystals by dielectric spectroscopy, Phys. Rev. Lett. 98 (2007) 037801.

[21] H. Takeuchi, Structure formation during the crystallization induction period of a short chain-molecule system: A molecular dynamics study, J. Chem. Phys. 109 (1998) 5614.
[22] S. Fujiwara, T. Sato, Molecular dynamics simulation of structural formation of short polymer chains, Phys. Rev. Lett. 80 (1998) 991.
[23] S. Fujiwara, T. Sato, Molecular dynamics simulation of structure formation of short chain molecules, J. Chem. Phys. 110 (1999) 9757.
[24] T. Shimizu, T. Yamamoto, Melting and crystallization in thin film of *n*-alkanes: A molecular dynamics simulation, J. Chem. Phys. 113 (2000) 3351.
[25] H. Meyer, F. Müller-Plathe, Formation of chain-folded structures in supercooled polymer melts, J. Chem. Phys. 115 (2001) 7807–7810.
[26] H. Meyer, F. Müller-Plathe, Formation of chain-folded structures in supercooled polymer melts examined by MD simulations, Macromolecules 35 (4) (2002) 1241–1252.
[27] D. Reith, H. Meyer, F. Müller-Plathe, Mapping atomistic to coarse-grained polymer models using automatic simplex optimization to fit structural properties, Macromolecules 34 (2001) 2335–2345.
[28] T. Vettorel, H. Meyer, J. Bashnagel, M. Fuchs, Structural properties of crystallizable polymer melts: Intrachain and interchain correlation functions, Phys. Rev. E 75 (2007) 041801.
[29] T. Vettorel, H. Meyer, Coarse graining of short polythylene chains for studying polymer crystallization, J. Chem. Theory Comput. 2 (2006) 616–629.
[30] K. Kremer, G.S. Grest, Dynamics of entangled linear polymer melts: A molecular-dynamics simulation, J. Chem. Phys. 92 (1990) 5057.
[31] K.L. Anderson, Simulation of thickening growth in polymer crystallisation, Polymer 41 (2000) 8849.
[32] J.P.K. Doye, D. Frenkel, Crystallization of a polymer on a surface, J. Chem. Phys. 109 (1998) 10033.
[33] J.P.K. Doye, D. Frenkel, Mechanism of thickness determination in polymer crystals, Phys. Rev. Lett. 81 (1998) 2160.
[34] Lammps molecular dynamics simulator, http://lammps.sandia.gov.
[35] http://tu-dresden.de/die_tu_dresden/zentrale_einrichtungen/zih.
[36] J.P. Hansen, I.R. McDonald, Theory of Simple Liquids, Academic Press, London, 1986.
[37] B. Heck, S. Siegenführ, G. Strobl, R. Thomann, A law controlling polymer recrystallization showing up in experiments on *s*-polypropylene, Polymer 48 (2007) 1352.
[38] M. Hikosaka, K. Amano, S. Rastogi, A. Keller, Lamellar thickening growth of an extended chain single crystal of polyethylene. 1. Pointers to a new crystallization mechanism of polymers, Macromolecules 30 (7) (1997) 2067–2074.
[39] G. Reiter, G. Castelein, J.-U. Sommer, Liquid-like morphological transformations in mono-lamellar polymer crystals, Phys. Rev. Lett. 86 (26) (2001) 5918.
[40] G. Reiter, J.-U. Sommer, Crystallization of adsorbed polymer monolayers, Phys. Rev. Lett. 80 (17) (1998) 3771.
[41] J.-U. Sommer, G. Reiter, Polymer crystallization in quasi-2 dimensions: Part II: Kinetic models, J. Chem. Phys. 112 (9) (2000) 4384–4393.
[42] J.-U. Sommer, G. Reiter, Morphogenesis of lamellar polymer crystals, Europhys. Lett. 56 (5) (2001) 755–761.